

# Structured Sparse Matrix Sketching based Detection for Media-based Modulation

Rupali Gupta, Bharath Shamasundar, and A. Chockalingam  
Department of ECE, Indian Institute of Science, Bangalore 560012

**Abstract**—In this paper, we consider media-based modulation (MBM) in a cyclic-prefixed single-carrier setting (CPSC-MBM) in inter-symbol interference channels and focus on low-complexity signal detection at the receiver. For this, we exploit the structured sparsity that is inherently present in CPSC-MBM signals. We formulate the sparse vector detection problem of interest as an equivalent sparse matrix detection problem, whose reconstruction complexity can be significantly less without incurring much loss in recovery performance. This technique of recovering sparse matrices, termed as *sparse matrix sketching*, applied to CPSC-MBM signal recovery is shown to achieve good bit error performance with significant complexity gains compared to the sparse vector detection approach.

**Keywords** – Media-based modulation, RF mirrors, sparse matrix sketching, FISTA, ADM.

## I. INTRODUCTION

Media-based modulation (MBM) is a recent channel modulation scheme which is shown to have promising theoretical and practical advantages [1]-[9]. MBM uses a single transmit radio frequency (RF) chain and one or more RF mirrors (parasitic elements) placed in the near field of the transmit antenna. In the ON state, an RF mirror reflects the RF signal and in the OFF state, it allows the signal to pass through. If there are  $m_{rf}$  RF mirrors, then there are  $2^{m_{rf}}$  ON and OFF combinations for these RF mirrors, called as mirror activation pattern (MAPs). The RF mirrors act as signal scatterers in the near field of the transmit antenna. Different MAPs create different near field geometry for the transmitted signal. Therefore,  $2^{m_{rf}}$  different MAPs create  $2^{m_{rf}}$  independent channels between the transmitter and the receiver. In a given channel use, one of the  $2^{m_{rf}}$  MAPs are selected using  $m_{rf}$  information bits. On the selected MAP, a symbol from a conventional modulation alphabet  $\mathbb{A}$  (e.g., QAM/PSK) is transmitted based on  $\log_2 |\mathbb{A}|$  bits. So, the achieved rate in MBM is  $\eta_{\text{MBM}} = m_{rf} + \log_2 |\mathbb{A}|$  bits per channel use (bpcu). MBM has several advantages compared to other single RF chain based schemes as highlighted below.

1) *Linear increase in rate with  $m_{rf}$* : From the achieved rate expression for MBM mentioned above, it can be seen that the rate increases linearly with the number of RF mirrors used. Whereas, a conventional system using a single RF chain and a modulation alphabet  $\mathbb{A}$  achieves a rate of  $\eta = \log_2 |\mathbb{A}|$  bpcu, which requires exponential increase in the modulation alphabet size to achieve linear increase in rate. Spatial modulation (SM) [10] also uses a single RF chain but uses multiple transmit antennas. An SM system achieves a rate of  $\eta_{\text{SM}} = \log_2 n_t + \log_2 |\mathbb{A}|$  bpcu. SM therefore requires an

exponential increase in either the transmit antennas or the modulation alphabet size to achieve linear increase in rate.

2) *Exponential growth in sparsity with  $m_{rf}$* : MBM signal vectors are inherently sparse. As will be discussed in Secs. II and III, the sparsity in MBM grows exponentially with the number of RF mirrors used. This is useful in low-complexity signal detection using sparse recovery algorithms. While SM signal vectors are also sparse, the sparsity in SM grows only linearly with the number of transmit antennas.

3) *Linear increase in capacity with  $n_r$* : MBM using one transmit antenna and  $n_r$  receive antennas has been shown to asymptotically achieve the capacity of  $n_r$  parallel AWGN channels [6],[9] (see Fig. 1 which shows the simulated MBM capacity plots as a function of  $m_{rf}$  for different  $n_r$ ).

Motivated by the above advantages of MBM over other single RF chain schemes, in the present work we focus on the low-complexity detection of MBM signals in ISI channels. MBM signal detection using sparse signal recovery techniques have been proposed in the recent literature [4],[8],[9],[11]. Recently, it is shown in the compressive sensing literature that if a sparse *vector recovery* problem can be converted to an equivalent sparse *matrix recovery* problem, then the recovery can be achieved at a significantly lesser complexity in the matrix form compared to that in the vector form without much compromise in the performance. This technique is termed as *sparse matrix sketching* [12],[13]. Towards this end, we consider cyclic-prefixed single-carrier MBM (CPSC-MBM) [5] systems in (ISI) channels and formulate the CPSC-MBM signal detection problem as a structured sparse matrix sketching problem, and propose two detection algorithms for CPSC-MBM signal detection based on sparse matrix sketching. It is shown that the proposed algorithms efficiently exploit the structured matrix form of CPSC-MBM signals and achieve low complexity detection with good performance.

The rest of the paper is organized as follows. The CPSC-MBM system model is presented in Sec. II. The proposed sparse matrix sketching based detection algorithms are presented in Sec. III. Section IV presents the bit error rate (BER) and complexity results for CPSC-MBM using the proposed algorithms. Conclusions are presented in Sec. V.

## II. SYSTEM MODEL

Consider an MBM system with a transmit antenna and  $m_{rf}$  RF mirrors surrounding it. The transmission in CPSC-MBM is carried out in frames. A transmission frame uses  $N$  time-slots to convey the data and  $L - 1$  time-slots for cyclic prefix (CP). Hence, the size of a frame is  $N + L - 1$  time-slots. An  $L$ -tap frequency-selective fading channel with exponential

This work was supported in part by the Visvesvaraya PhD Scheme of the Ministry of Electronics & IT, Government of India, J. C. Bose National Fellowship, Department of Science and Technology, Government of India, and the Intel India Faculty Excellence Program.

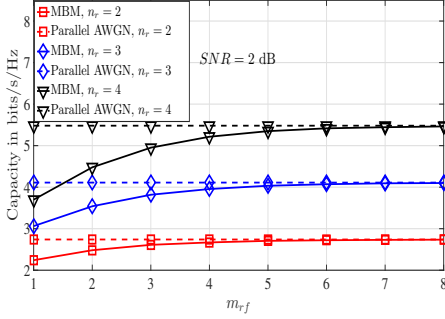


Fig. 1: MBM capacity as a function of  $m_{rf}$  and  $n_r$  at SNR = 2 dB.

power-delay profile is considered. In each of the  $N$  channel uses of the data part of the frame, one of the  $N_m \triangleq 2^{m_{rf}}$  MAPs is selected using  $m_{rf}$  information bits. Using the selected MAP, a symbol from a conventional alphabet  $\mathbb{A}$  (e.g., QAM/PSK) is transmitted based on  $\log_2 |\mathbb{A}|$  bits. The achieved rate of CPSC-MBM system in bpcu is therefore given by  $\eta = \frac{N}{N+L-1} \{m_{rf} + \log_2 |\mathbb{A}|\}$  bpcu.

Let  $\mathbb{A}_0 \triangleq \mathbb{A} \cup 0$ . The MBM signal set,  $\mathbb{S}_{\text{MBM}}$ , is the set of  $N_m \times 1$ -sized MBM signal vectors given by

$$\mathbb{S}_{\text{MBM}} = \{s_{k,p} \in \mathbb{A}_0^{N_m}; k = 1, \dots, N_m; p = 1, \dots, |\mathbb{A}|\}$$

$$\text{s.t. } s_{k,p} = [0, \dots, 0, \underbrace{s_p}_{k\text{th entry}}, 0, \dots, 0]^T, s_p \in \mathbb{A}, \quad (1)$$

where  $k$  is the MAP index. The receiver has  $n_r$  receive antennas. The channel is assumed to remain constant for one frame duration and is assumed to be known perfectly at the receiver. In each of the  $N$  channel uses of the data part of the frame, an MBM signal vector from  $\mathbb{S}_{\text{MBM}}$  is transmitted. Let  $\mathbf{x}_j \in \mathbb{S}_{\text{MBM}}$  denote the  $N_m \times 1$  transmitted signal vector in the  $j$ th channel use,  $-L \leq j \leq N-1$ . At the receiver, after CP removal, the  $Nn_r \times 1$  received signal vector is given by

$$\mathbf{y} = \mathbf{H}\mathbf{x} + \mathbf{n}, \quad (2)$$

where  $\mathbf{n} \sim \mathcal{CN}(0, \sigma^2 \mathbf{I}_{Nn_r})$  is the  $Nn_r \times 1$  noise vector,  $\mathbf{x}$  is the  $NN_m \times 1$  vector which forms the data part of the frame, given by  $\mathbf{x} = [\mathbf{x}_0^T \mathbf{x}_1^T \dots \mathbf{x}_{N-1}^T]^T$ , and  $\mathbf{H}$  is the  $Nn_r \times NN_m$  equivalent block circulant matrix, given by

$$\mathbf{H} = \text{circ}[\mathbf{H}_0, \mathbf{H}_1, \dots, \mathbf{H}_{L-1}, \mathbf{0}, \dots, \mathbf{0}], \quad (3)$$

where  $\mathbf{H}_l$  is the  $n_r \times N_m$  channel gain matrix corresponding to the  $l$ th multipath whose  $(i, k)$ th entry is  $h_{i,k}^{(l)}$ , where  $h_{i,k}^{(l)}$  denotes the channel gain from the transmit antenna to the  $i$ th receive antenna for the  $l$ th path when  $k$ th MAP is used,  $i = 1, \dots, n_r$ ,  $k = 1, \dots, N_m$ ,  $l = 0, \dots, L-1$ . The power-delay profile is assumed to follow an exponential decay model, i.e.,  $\mathbb{E}[|h_{i,k}^{(l)}|^2] = e^{-l}$ ,  $l = 0, 1, \dots, L-1$ . The maximum likelihood (ML) detection rule for the system model (2) is given by

$$\hat{\mathbf{x}} = \underset{\mathbf{x} \in \mathbb{S}_{\text{MBM}}}{\text{argmin}} \|\mathbf{y} - \mathbf{H}\mathbf{x}\|^2. \quad (4)$$

The detection complexity in (4) is  $\mathcal{O}(N^2 N_m n_r 2^{(N m_{rf} + N \log_2 |\mathbb{A}|)})$ , which is exponential in the frame size  $N$ , making it infeasible for large  $N$ .

### III. DETECTION USING SPARSE MATRIX SKETCHING

From (1), the MBM signal vectors can be seen to have only one non-zero entry out of the  $N_m = 2^{m_{rf}}$  entries. Since the CPSC-MBM signal vector is the concatenation of  $N$  MBM vectors, it is also sparse with the same sparsity factor. Specifically, CPSC-MBM signal vector is a sparse  $NN_m \times 1$  vector with only one non-zero entry in every  $N_m$ -length MBM subvector. The sparsity along with this additional structure can be exploited to design efficient detectors using structured compressive sensing based sparse recovery techniques.

#### A. CPSC-MBM received signal in alternate form

We express the block circulant matrix  $\mathbf{H}$  in (3) as

$$\mathbf{H} = (\mathbf{F}^H \otimes \mathbf{I}_{n_r}) \mathbf{D} (\mathbf{F} \otimes \mathbf{I}_{N_m}), \quad (5)$$

where  $\otimes$  denotes the Kronecker product,  $(\cdot)^H$  denotes the Hermitian operation, and  $\mathbf{F}$  is the DFT matrix, given by

$$\mathbf{F} = 1/\sqrt{N} \begin{bmatrix} \rho_{0,0} & \rho_{0,1} & \dots & \rho_{0,N-1} \\ \rho_{1,0} & \rho_{1,1} & \dots & \rho_{1,N-1} \\ \vdots & \vdots & \ddots & \vdots \\ \rho_{N-1,0} & \rho_{N-1,1} & \dots & \rho_{N-1,N-1} \end{bmatrix},$$

where  $\rho_{m,n} = \exp(-\frac{j2\pi mn}{N})$ , and  $\mathbf{D}$  is a block diagonal matrix given by

$$\mathbf{D} = \text{diag}[\mathbf{D}_0, \mathbf{D}_1, \dots, \mathbf{D}_{L-1}] \quad \text{s.t.} \quad \mathbf{D}_l = \sum_{i=1}^{L-1} \rho_{i,l} \mathbf{H}_i. \quad (6)$$

From (5), we can write

$$\mathbf{H}\mathbf{x} = (\mathbf{F}^H \otimes \mathbf{I}_{n_r}) \mathbf{D} (\mathbf{F} \otimes \mathbf{I}_{N_m}) \mathbf{x},$$

$$= (\mathbf{F}^H \otimes \mathbf{I}_{n_r}) \begin{bmatrix} \mathbf{D}_0 (\mathbf{f}_0 \otimes \mathbf{I}_{N_m}) \mathbf{x} \\ \mathbf{D}_1 (\mathbf{f}_1 \otimes \mathbf{I}_{N_m}) \mathbf{x} \\ \vdots \\ \mathbf{D}_{N-1} (\mathbf{f}_{N-1} \otimes \mathbf{I}_{N_m}) \mathbf{x} \end{bmatrix}, \quad (7)$$

where  $\mathbf{f}_i$  denotes the  $i$ th row of  $\mathbf{F}$ . Let  $\mathbf{X} = [\mathbf{x}_0 \mathbf{x}_1 \dots \mathbf{x}_{N-1}]$  be the  $N_m \times N$  matrix such that  $\mathbf{x} = \text{vec}(\mathbf{X}) = [\mathbf{x}_0^T \mathbf{x}_1^T \dots \mathbf{x}_{N-1}^T]^T$ . Now, (7) can be further simplified as

$$\mathbf{H}\mathbf{x} = (\mathbf{F}^H \otimes \mathbf{I}_{n_r}) \begin{bmatrix} \mathbf{D}_0 \mathbf{X} \mathbf{f}_0^T \\ \vdots \\ \mathbf{D}_{N-1} \mathbf{X} \mathbf{f}_{N-1}^T \end{bmatrix}. \quad (8)$$

Using the property of the Kronecker product  $\text{vec}(\mathbf{A}\mathbf{X}\mathbf{B}^T) = (\mathbf{B} \otimes \mathbf{A})\text{vec}(\mathbf{X})$  in (8), the received signal vector in (2) can be written in the alternate form as an  $n_r \times N$  matrix  $\mathbf{Y} \triangleq [\mathbf{y}_0 \mathbf{y}_1 \dots \mathbf{y}_{N-1}]$  as

$$\mathbf{Y} = \mathbf{I}_{n_r} [\mathbf{D}_0 \mathbf{X} \mathbf{f}_0^T \mathbf{D}_1 \mathbf{X} \mathbf{f}_1^T \dots \mathbf{D}_N \mathbf{X} \mathbf{f}_{N-1}^T] \mathbf{F}^{HT} + \mathbf{N}$$

$$= [\mathbf{D}_0 \mathbf{X} \mathbf{f}_0^T \mathbf{D}_1 \mathbf{X} \mathbf{f}_1^T \dots \mathbf{D}_{N-1} \mathbf{X} \mathbf{f}_{N-1}^T] \mathbf{F}^* + \mathbf{N}, \quad (9)$$

where  $\mathbf{N} \in \mathbb{C}^{n_r \times N}$  is the noise matrix with  $\mathbf{N}_{i,j} \sim \mathcal{CN}(0, \sigma^2)$ , and  $\mathbf{F}^*$  denotes the element-wise conjugation of matrix  $\mathbf{F}$ .

### B. Formulation of the signal detection problem

A sparse matrix sketching problem is to solve

$$\min_{\mathbf{X}} \|\mathbf{X}\|_1 \quad \text{s.t.} \quad \mathbf{Y} = \mathbf{A}\mathbf{X}\mathbf{B}^T + \mathbf{N}, \quad (10)$$

where  $\mathbf{Y}$  is the observation matrix,  $\mathbf{A}$  and  $\mathbf{B}$  are known matrices [13]. We use the alternate form of the CPSC-MBM received signal in (9) and formulate the detection problem as sparse matrix sketching problem in a slightly modified form compared to (10). Specifically, the CPSC-MBM signal detection problem can be formulated as a structured sparse matrix sketching problem as

$$\min_{\mathbf{X}} \|\mathbf{X}\|_1 \quad \text{s.t.} \quad (11)$$

a)  $\tilde{\mathbf{Y}} = f(\mathbf{X}) + \tilde{\mathbf{N}}$ , b)  $\|\mathbf{x}_i\|_0 = 1 \quad \forall i = 0, 1, \dots, N-1$ ,

where  $\tilde{\mathbf{Y}} = \mathbf{Y}(\mathbf{F}^*)^{-1} = f(\mathbf{X}) + \tilde{\mathbf{N}}$ , with  $\mathbf{Y}$  as in (9),  $f(\mathbf{X}) = [\mathbf{D}_0\mathbf{X}\mathbf{f}_0^T \quad \mathbf{D}_1\mathbf{X}\mathbf{f}_1^T \quad \dots \quad \mathbf{D}_{N-1}\mathbf{X}\mathbf{f}_{N-1}^T]$ ,  $\tilde{\mathbf{N}} = \mathbf{N}(\mathbf{F}^*)^{-1}$ , and  $\mathbf{x}_i$  is the  $i$ th column of  $\mathbf{X}$ . We now make a few remarks on the above formulation.

*Remark 1:* Although the formulation in (11) involves reconstruction of a sparse matrix, it is different from the canonical form of the matrix sketching problem in (10) in two aspects. Firstly, the form of the observation matrix as given in a) of (11) is specific to CPSC-MBM and is different from that in (10). Secondly, the canonical form in (10) has no additional structure in the problem, whereas the constraint b) in (11) requires only one non-zero to be reconstructed in each column of the sparse matrix  $\mathbf{X}$ .

*Remark 2:* The formulation in (11) is different from the conventional sparse *vector* recovery approach. Specifically, the sparse vector recovery formulation is based on the system model in (2) and is given by

$$\min \|\mathbf{x}\|_1 \quad \text{s.t.} \quad \mathbf{y} = \mathbf{H}\mathbf{x} + \mathbf{n}, \quad \|\mathbf{x}_i\|_0 = 1, \forall i = 0, \dots, N-1. \quad (12)$$

In the following subsections, we propose two algorithms to solve (11) based on sparse matrix sketching. The first algorithm is based on fast iterative shrinkage-thresholding algorithm (FISTA) [14], with extensions and modifications to suit the specific structure of the problem in (11). We call this algorithm as ‘MBM matrix FISTA’ (MBM-MFISTA). We also propose a matrix sketching algorithm which builds on alternating direction method (ADM) [15] to enable matrix recovery. We call this algorithm as ‘MBM matrix ADM’ (MBM-MADM).

### C. Signal detection using MBM-MFISTA

To solve the optimization problem in (11), we consider the following regularized  $l_1$ -norm optimization problem:

$$\min_{\mathbf{X}} \left\{ \frac{1}{2} \|\tilde{\mathbf{Y}} - f(\mathbf{X})\|_F^2 + \lambda \|\mathbf{X}\|_1 \right\}, \quad (13)$$

where  $\lambda$  is regularization parameter. (13) can be written as

$$\min_{\mathbf{X}} \left\{ \frac{1}{2} \sum_{i=0}^{N-1} \|\tilde{\mathbf{y}}_i - \mathbf{D}_i\mathbf{X}\mathbf{f}_i^T\|_2^2 + \lambda \|\mathbf{X}\|_1 \right\}, \quad (14)$$

where  $\tilde{\mathbf{y}}_i$  is the  $i$ th column of the matrix  $\tilde{\mathbf{Y}}$ . For a complex matrix  $\mathbf{A} \in \mathbb{C}^{M \times N}$ , the equivalent matrix in the real form is

### Algorithm 1 Listing of proposed MBM-MFISTA

- 1) **Input:**  $[\tilde{\mathbf{y}}_{r_i}]_{i=0}^{N-1}$ ,  $[\mathbf{D}_{r_i}]_{i=0}^{N-1}$ ,  $[\mathbf{f}_{r_i}]_{i=0}^{N-1}$
- 2) **Initialization:**  $\mathbf{X}_r^0 = 0$ ,  $\mathbf{X}_r^1 = 0$ ,  $t_0 = 1$ ,  $t_1 = 1$ ,  $n = 1$ ,  $\lambda_1 > 0$ ,  $\bar{\lambda} > 0$ ,  $\alpha \in (0, 1)$ ,  $L_f$ ,  $\tilde{\mathbf{X}} = N_m \times N$  zero matrix.
- 3) **while** not converged **do**
- 4)  $\mathbf{R}^n = \mathbf{X}_r^n + \frac{t_{n-1}-1}{t_n}(\mathbf{X}_r^n - \mathbf{X}_r^{n-1})$
- 5)  $\mathbf{V}^n = \mathbf{R}^n - \frac{1}{L_f} \sum_{i=0}^{N-1} \mathbf{D}_{r_i}^T (\mathbf{D}_{r_i} \mathbf{R}^n \mathbf{f}_{r_i}^T - \tilde{\mathbf{y}}_{r_i}) \mathbf{f}_{r_i}$
- 6)  $\mathbf{X}_r^{n+1} = \text{soft}(\mathbf{V}^n, \frac{\lambda_n}{L_f})$
- 7)  $t_{n+1} = \frac{1 + \sqrt{4t_n^2 + 1}}{2}$
- 8)  $\lambda_{n+1} = \max(\alpha \lambda_n, \bar{\lambda})$
- 9)  $n = n + 1$
- 10) **end while**
- 11) Convert  $\mathbf{X}_r^n$  to complex form  $\mathbf{X}^n$
- 12)  $\{p_1, p_2, \dots, p_N\} = S_x(\mathbf{X}^n)$
- 13)  $\tilde{\mathbf{X}}(p_k, k) = \underset{s \in \mathbb{A}}{\text{argmin}} \|\mathbf{X}^n(p_k, k) - s\|^2$ ,  $k = 1, 2, \dots, N$
- 14) **Output:**  $\tilde{\mathbf{X}}$

$$\mathbf{A}_r = \begin{bmatrix} \text{Re}(\mathbf{A}) & -\text{Im}(\mathbf{A}) \\ \text{Im}(\mathbf{A}) & \text{Re}(\mathbf{A}) \end{bmatrix}.$$

The optimization problem in (14) in real form is

$$\min_{\mathbf{X}_r} \left\{ \frac{1}{2} \sum_{i=0}^{N-1} \|\tilde{\mathbf{y}}_{r_i} - \mathbf{D}_{r_i} \mathbf{X}_r \mathbf{f}_{r_i}^T\|_F^2 + \lambda \|\mathbf{X}_r\|_1 \right\}. \quad (15)$$

For solving (15), we consider the approach in [12] which generalizes FISTA for sparse matrix recovery. However, necessary changes are made to satisfy the constraints in (11). The proposed MBM-MFISTA listing is given in **Algorithm 1**.

In **Algorithm 1**, steps 1 to 4 and 6 to 10 are same as those of MFISTA in [12]. The main modifications are in steps 5 and 12 which account for the constraints in (11). Specifically, step 5 is the gradient step specific to the form of the CPSC-MBM observation matrix in (9), which is taken care in the constraint a) of (11). In step 12,  $S_x$  selects one position in each column of  $\mathbf{X}^n$  which contains the entry with highest absolute value in that column. Then, all the entries of  $\mathbf{X}^n$  other than the ones selected by  $S_x$  are set to zero. This is taken care in steps 2 (initialization of  $\tilde{\mathbf{X}}$ ) and 12, which ensure only one non-zero element in each column of the reconstructed CPSC-MBM matrix, thus satisfying the constraint b) in (11). Finally, the reconstructed non-zeros are mapped to the valid symbols in  $\mathbb{A}$  in step 13. In the algorithm,  $L_f$  is the Lipschitz constant of  $\nabla F(\mathbf{X}_r)$ , where  $F(\mathbf{X}_r) = \frac{1}{2} \sum_{i=0}^{N-1} \|\tilde{\mathbf{y}}_{r_i} - \mathbf{D}_{r_i} \mathbf{X}_r \mathbf{f}_{r_i}^T\|_F^2$ ,  $\text{soft}(\mathbf{A}^n, a) = \text{sgn}(\mathbf{A}_{i,j}^n) (|\mathbf{A}_{i,j}^n| - a)_+$ ,  $\forall (i, j)$ .

*Complexity:* The computational complexity of **Algorithm 1** is governed by step 5, which involves computing  $\sum_{i=0}^{N-1} \mathbf{D}_{r_i}^T (\mathbf{D}_{r_i} \mathbf{R}^n \mathbf{f}_{r_i}^T - \tilde{\mathbf{y}}_{r_i}) \mathbf{f}_{r_i}$  and has the complexity of  $\mathcal{O}(8N^2 N_m n_r + 8N^2 N_m^2 + 24N^2 N_m + 8N N_m n_r)$ , which is mainly dominated by the  $\mathcal{O}(8N^2 N_m^2)$  term. The complexity of vector FISTA [14] is  $\mathcal{O}(8N^3 N_m^2 n_r + 4N^2 N_m + 4N^2 N_m n_r)$  which is dominated by the  $\mathcal{O}(8N^3 N_m^2 n_r)$ . So, the complexity of MBM-MFISTA is less than that of vector FISTA by a factor of  $N n_r$ .

### D. Signal detection using MBM-MADM

In this subsection, we present the proposed MBM-MADM which is an extension of ADM [15] to the matrix case. In

order to extend ADM to sparse matrix recovery, we introduce the auxiliary term  $\mathbf{Z}$  in (15), which results in the following optimization problem:

$$\min_{\mathbf{X}_r, \mathbf{Z}} \left\{ \frac{1}{2} \sum_{i=0}^{N-1} \|\tilde{\mathbf{y}}_{r_i} - \mathbf{D}_{r_i} \mathbf{Z} \mathbf{f}_{r_i}^T\|_F^2 + \lambda \|\mathbf{X}_r\|_1 \right\} \text{ s.t } \mathbf{X}_r = \mathbf{Z}. \quad (16)$$

The augmented Lagrangian function of (16) is then given by

$$\begin{aligned} \operatorname{argmin}_{\mathbf{X}_r, \mathbf{Z}, \Lambda} L(\mathbf{X}_r, \mathbf{Z}, \Lambda) &= \frac{1}{2} \sum_{i=0}^{N-1} \|\tilde{\mathbf{y}}_{r_i} - \mathbf{D}_{r_i} \mathbf{Z} \mathbf{f}_{r_i}^T\|_F^2 + \lambda \|\mathbf{X}_r\|_1 \\ &+ \operatorname{Tr}(\Lambda^T (\mathbf{Z} - \mathbf{X}_r)) + \frac{\rho}{2} \|\mathbf{Z} - \mathbf{X}_r\|_F^2, \end{aligned} \quad (17)$$

where  $\Lambda \in \mathbb{R}^{2N_m \times 2N}$  is the Lagrange multiplier matrix,  $\rho$  is the penalty parameter, and  $\operatorname{Tr}(\cdot)$  denotes the trace operator. Now, the ADM iterations are achieved by solving the following single (matrix) variable optimization problems and the Lagrange multiplier matrix update:

$$\mathbf{Z}^{n+1} = \operatorname{argmin}_{\mathbf{Z}} L(\mathbf{X}_r^n, \mathbf{Z}, \Lambda^n), \quad (18a)$$

$$\mathbf{X}_r^{n+1} = \operatorname{argmin}_{\mathbf{X}_r} L(\mathbf{X}_r, \mathbf{Z}^{n+1}, \Lambda^n), \quad (18b)$$

$$\Lambda^{n+1} = \Lambda^n + \rho(\mathbf{Z}^{n+1} - \mathbf{X}_r^{n+1}). \quad (18c)$$

The optimization problem (18a) is solved using the accelerated gradient method [16] for  $K$  iterations, with the  $(k+1)$ th iteration given by

$$\mathbf{Z}^{k+1} = \mathbf{U}^k - \eta \nabla f(\mathbf{U}^k) \quad (19a)$$

$$\mathbf{U}^{k+1} = \mathbf{Z}^{k+1} - \frac{k}{k+3} (\mathbf{Z}^{k+1} - \mathbf{Z}^k), \quad (19b)$$

where  $f(\mathbf{U}^k) = \left\{ \sum_{i=0}^{N-1} \|\tilde{\mathbf{y}}_{r_i} - \mathbf{D}_{r_i} \mathbf{U}^k \mathbf{f}_{r_i}^T\|_F^2 + \operatorname{Tr}(\Lambda^T (\mathbf{U}^k - \mathbf{X}_r)) + \frac{\rho}{2} \|\mathbf{U}^k - \mathbf{X}_r\|_F^2 \right\}$ . The solution to (18a) is then  $\mathbf{Z}^{n+1} = \mathbf{Z}^K$ . The optimization problem (18b) is equivalent to

$$\operatorname{argmin}_{\mathbf{X}_r} \lambda \|\mathbf{X}_r\|_1 + \frac{\rho}{2} \|\mathbf{Z}^{n+1} - \mathbf{X}_r + \Lambda^n / \rho\|_F^2, \quad (20)$$

which can be solved by soft thresholding as

$$\mathbf{X}_r^{n+1} = \operatorname{soft}(\mathbf{Z}^{n+1} + \Lambda^n / \rho, \lambda / \rho). \quad (21)$$

The Lagrange multiplier matrix is then updated in (18c) by using the solutions of (18a) and (18b). The iterations in (18a), (18b), and (18c) are continued till a maximum number of iterations is reached.

The listing of the proposed MBM-MADM is given in **Algorithm 2**. The steps 1 to 16 shown in the listing achieve the iterative procedure discussed above. Although the iterative procedure results in the sparse matrix reconstruction, the structure of the CPSC-MBM as imposed by the condition  $b)$  of (11) has to be separately taken care of. This is achieved by restricting one non-zero per each column of the reconstructed sparse matrix, which is shown in step 17 of the algorithm, where  $S_x$  is as defined before. Finally, the reconstructed non-zeros are mapped to the valid symbols from  $\mathbb{A}$  in step 18. In the algorithm,  $\operatorname{soft}(\mathbf{A}^n, a) = \operatorname{sgn}(\mathbf{A}_{i,j}^n) (|\mathbf{A}_{i,j}^n| - a)_+, \forall (i, j)$ .

*Complexity:* The complexity of **Algorithm 2** is governed by the gradient descent step, where the computation of  $\sum_{i=0}^{N-1} \mathbf{D}_{r_i}^T (\mathbf{D}_{r_i} \mathbf{U}^k \mathbf{f}_{r_i}^T - \tilde{\mathbf{y}}_{r_i}) \mathbf{f}_{r_i}$  has a complexity of

---

### Algorithm 2 Listing of proposed MBM-MADM

---

- 1) **Input:**  $[\tilde{\mathbf{y}}_{r_i}]_{i=0}^{N-1}, [\mathbf{D}_{r_i}]_{i=0}^{N-1}, [\mathbf{f}_{r_i}]_{i=0}^{N-1}$
  - 2) **Initialize:**  $\mathbf{X}_r^0 = \mathbf{0}, \mathbf{Z}^0 = \mathbf{0}, \Lambda^0 = \mathbf{0}, n = 1, \lambda = 2, \rho^0 = 0.1, \bar{\rho} = 5, \alpha = 1.1, \tilde{\mathbf{X}} = N_m \times N$  zero matrix
  - 3) **while** not converged **do**
  - 4)  $\mathbf{V}^0 = \mathbf{Z}^n, \mathbf{U}^0 = \mathbf{0}, k = 1, \eta > 0$
  - 5) **for**  $k : 1 \rightarrow K$
  - 6)  $\mathbf{V}^{k+1} = \mathbf{U}^k - \eta \sum_{i=0}^{N-1} \mathbf{D}_{r_i}^T (\mathbf{D}_{r_i} \mathbf{U}^k \mathbf{f}_{r_i}^T - \tilde{\mathbf{y}}_{r_i}) \mathbf{f}_{r_i} - \Lambda^n - \rho^n (\mathbf{U}^k - \mathbf{X}_r)$
  - 7)  $\mathbf{U}^{k+1} = \mathbf{V}^{k+1} - \frac{k}{k+3} (\mathbf{V}^{k+1} - \mathbf{V}^k)$
  - 8)  $k = k + 1$
  - 9) **end for**
  - 10)  $\mathbf{Z}^{n+1} = \mathbf{V}^K$
  - 11)  $\mathbf{X}_r^{n+1} = \operatorname{soft}(\mathbf{Z}^{n+1} + \Lambda^n / \rho^n, \lambda / \rho^n)$
  - 12)  $\Lambda^{n+1} = \Lambda^n + \rho^n (\mathbf{Z}^{n+1} - \mathbf{X}_r^{n+1})$
  - 13)  $\rho^{n+1} = \min(\alpha \rho^n, \bar{\rho})$
  - 14)  $n = n + 1$
  - 15) **end while**
  - 16) Convert  $\mathbf{X}_r^n$  to complex form  $\mathbf{X}^n$
  - 17)  $\{p_1, p_2, \dots, p_N\} = S_x(\mathbf{X}^n)$
  - 18)  $\tilde{\mathbf{X}}(p_t, t) = \operatorname{argmin}_{s \in \mathbb{A}} \|\mathbf{X}^n(p_t, t) - s\|^2, t = 1, 2, \dots, N$
  - 19) **Output:**  $\tilde{\mathbf{X}}$
- 

$O(8N^2 N_m n_r + 8N^2 N_m^2 + 24N^2 N_m + 8NN_m n_r)$  operations. Further, the accelerated gradient descent is performed for  $K$  iterations. Therefore, the overall complexity is  $O(8N^2 N_m n_r K + 8N^2 N_m^2 K + 24N^2 N_m K + 8NN_m n_r K)$ , which is dominated by  $O(8N^2 N_m^2 K)$ . On the other hand, the complexity of the vector ADM is  $O(8N^3 N_m^3)$  [15]. Therefore, the complexity of vector ADM is cubic in  $NN_m$ , while it is only quadratic in  $NN_m$  for MBM-MADM.

## IV. RESULTS AND DISCUSSIONS

In this section, we present numerical results on the convergence, complexity, and bit error rate (BER) performance of the proposed algorithms. Figures 2(a) and 2(b) show the normalized mean squared error (NMSE),  $\|\mathbf{X} - \tilde{\mathbf{X}}\|_F^2 / \|\mathbf{X}\|_F^2$ , as a function of number of iterations using MBM-MFISTA and MBM-MADM, respectively. We also show the NMSE of the equivalent structured sparse vector algorithms ‘MBM vector FISTA’ (MBM-VFISTA) and ‘MBM vector ADM’ (MBM-VADM) for comparison. It can be seen that the NMSE decreases with the increase in number of iterations and becomes flat after certain number of iterations, which is about 50 and 75 iterations for MBM-MFISTA and MBM-MADM, respectively. These values are used as the maximum number of iterations in the BER simulations reported next.

In Fig. 3, we plot the BER performance of CPSC-MBM using MBM-MFISTA and MBM-MADM algorithms for two system configurations. We also show the detection performance with MBM-VFISTA and MBM-VADM. The BER performance with vector approximate message passing (VAMP) as in [11] is also shown for comparison. It can be seen that CPSC-MBM performance with MBM-MFISTA is slightly better than that with MBM-MADM. Further, the performance of CPSC-MBM using MBM-MFISTA is almost the same as

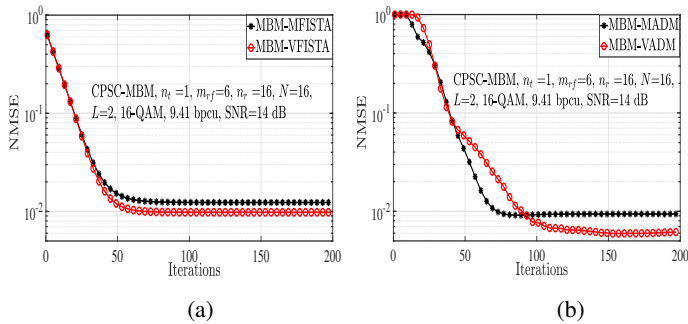


Fig. 2: NMSE as function of number of iterations with MBM-VFISTA, MBM-MADDM, MBM-VADM, and VAMP.

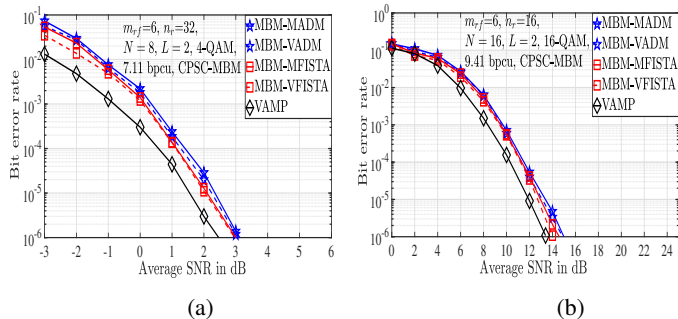


Fig. 3: BER performance of CPSC-MBM using MBM-VFISTA (proposed), MBM-MADDM (proposed), MBM-VADM, and VAMP [11].

that using MBM-VFISTA, and the performance of CPSC-MBM using MBM-MADDM is very close to that using MBM-VADM. Also, the BER performance with VAMP is slightly better than that with MBM-MFISTA. However, as we illustrate next, the complexities of MBM-MFISTA and MBM-MADDM are less than that of VAMP.

In Figs. 4(a) and 4(b), we show the complexity of the proposed detectors as  $m_{rf}$  and  $N$  are varied, respectively. The complexity of MBM-VFISTA, MBM-VADM, and VAMP are shown for comparison. It can be seen that the complexity of the proposed MBM-MFISTA and MBM-MADDM are considerably less than those of MBM-VFISTA, MBM-VADM, and VAMP.

Next, we present a BER and complexity comparison of the proposed detection algorithms with optimal ML detection Figs. 5(a) and 5(b). From these figures, it can be seen that the proposed algorithms achieve a BER performance within 1.5 dB of the optimal ML detector. It can be further observed from Fig. 5(b) that the complexity of the proposed detectors is lesser than that of the ML detector.

## V. CONCLUSIONS

We considered the problem of low complexity detection for CPSC-MBM signals in ISI channels. We proposed two structured sparse matrix sketching based detection algorithms by extending the vector FISTA and vector ADM algorithms. Simulation results showed that the proposed detectors trade off a small loss in BER to a significant reduction in complexity.

## REFERENCES

[1] A. K. Khandani, "Media-based modulation: A new approach to wireless transmission," in *Proc. IEEE ISIT'2013*, Jul. 2013, pp. 3050-3054.

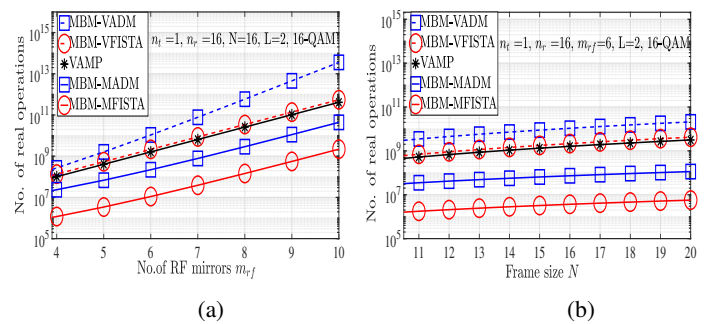


Fig. 4: Complexity of MBM-MFISTA (proposed), MBM-MADDM (proposed), MBM-VFISTA, MBM-VADM, and VAMP [11].

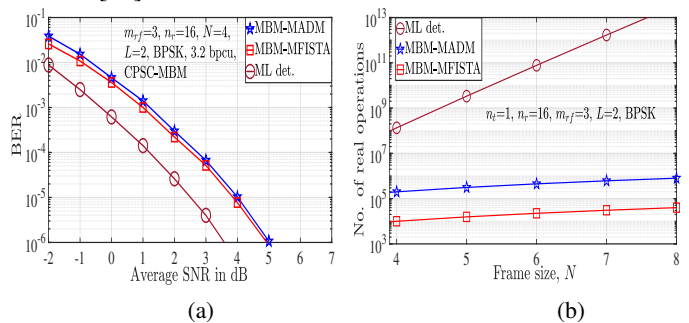


Fig. 5: BER and complexity comparison of CPSC-MBM using optimal ML detection and the proposed detection algorithms.

[2] Y. Naresh and A. Chockalingam, "On media-based modulation using RF mirrors," *IEEE Trans. Veh. Tech.*, vol. 66, pp. 4967-4983, Jun. 2017.

[3] E. Basar and I. Altunbas, "Space-time channel modulation," *IEEE Trans. Veh. Tech.*, vol. 66, no. 8, pp. 7609-7614, Aug. 2017.

[4] L. Zhang, M. Zhao, and L. Li, "Low-complexity multi-user detection for MBM in uplink large-scale MIMO systems," *IEEE Commun. Lett.*, vol. 22, no. 8, pp. 1568-1571, Aug. 2018.

[5] S. Jacob and A. Chockalingam, "Single-carrier media-based modulation in ISI channels," in *Proc. NCC'2017*, Mar. 2017.

[6] A. K. Khandani, "Media-based modulation: Converting static Rayleigh fading to AWGN," in *Proc. IEEE ISIT'2014*, Jul. 2014, pp. 1549-1553.

[7] B. Shamasundar, K. M. Krishnan, T. L. Narasimhan, and A. Chockalingam, "MAP-index coded media-based modulation," *IEEE Commun. Lett.*, vol. 22, no. 12, pp. 2455-2458, Dec. 2018.

[8] A. Bandi and C. R. Murthy, "Structured sparse recovery algorithms for data decoding in media based modulation," in *Proc. IEEE ICC'2017*, May 2017, pp. 1-6.

[9] B. Shamasundar, S. Jacob, T. L. Narasimhan, and A. Chockalingam, "Media-based modulation for the uplink in massive MIMO systems," *IEEE Trans. Veh. Tech.*, vol. 67, no. 9, pp. 8169-8183, Sep. 2018.

[10] M. Di Renzo, H. Haas, A. Ghayeb, S. Sugiura, and L. Hanzo, "Spatial modulation for generalized MIMO: challenges, opportunities and implementation," *Proc. of the IEEE*, vol. 102, no. 1, pp. 56-103, Jan. 2014.

[11] L. Liu and W. Yu, "Massive connectivity with massive MIMO - part I: device activity detection and channel estimation," *IEEE Trans. Signal Process.*, vol. 66, no. 11, pp. 2933-2946, Jun. 2018.

[12] T. Wimalajeewa, Y. C. Eldar, and P. K. Varshney, "Recovery of sparse matrices via matrix sketching," *arXiv preprint arXiv:1311.2448*, 2013.

[13] G. Dasarthy, P. Shah, B. N. Bhaskar, and R. D. Nowak, "Sketching sparse matrices, covariances, and graphs via tensor products," *IEEE Trans. Inf. Theory*, vol. 61, no. 3, pp. 1373-1388, Mar. 2015.

[14] A. Beck and M. Teboulle, "Fast iterative shrinkage-thresholding algorithm for linear inverse problems," *SIAM Jour. Imaging Sciences*, vol. 2, no. 1, pp. 183-202, 2009.

[15] J. Yang and Y. Zhang, "Alternating direction algorithms for  $l_1$ -problems in compressive sensing," *SIAM Jour. Scientific Computing*, vol. 33, no. 1, pp. 250-278, 2011.

[16] Y. Nesterov, "A method of solving a convex programming problem with convergence rate  $O(1/k^2)$ ," *Soviet Mathematics Doklady*, vol. 27, no. 2, pp. 372-376, 1983.